Journal of Power Sources 184 (2008) 284–287

Contents lists available at ScienceDirect

Journal of Power Sources

journal homepage: www.elsevier.com/locate/jpowsour

Short communication

Design of TiO_2 nanotube array-based water-splitting reactor for hydrogen generation

Eun Young Kim, Jong Hyeok Park, Gui Young Han*

Department of Chemical Engineering, Sungkyunkwan University, Suwon 440-746, Republic of Korea

ARTICLE INFO

Article history:
Received 28 March 2008
Received in revised form 17 April 2008
Accepted 12 May 2008
Available online 29 May 2008

Keywords:
Water splitting
TiO_2 nanotube
Hydrogen
Photoanode

ABSTRACT

A water-splitting reactor yielding hydrogen and oxygen was designed with a titanium oxide (TiO_2) nanotube array photoelectrode vertically grown on a titanium substrate. The TiO_2 nanotube arrays were made by the method of anodization and annealed in an oxygen atmosphere. Hydrogen gas was collected from the reactor and the exact amount of hydrogen gas evolved from the photoanode was analyzed. The relationship between the amount of hydrogen evolution and three key factors, viz. the tube length, tube structure and crystal structure, was investigated.

1. Introduction

Water photolysis is the ideal technology for human beings to use in the future because of its advantages of the direct usage of sunlight and water and virtually unlimited resources. Especially, water decomposition technology with photocatalysts consisting of titanium oxide (TiO_2) nanoparticles has great potential to produce low priced and environmentally friendly hydrogen in the future [1–4]. However, presently, the conversion efficiency of solar–hydrogen energy is too low for it to be commercialized. The major drawback is the high recombination possibility of photo-generated electrons in the case of nanoparticle dispersed systems [5].

To overcome this problem, many researchers are investigating photoelectrochemical methods, wherein electron–hole pairs are generated when the photoelectrode absorbs photon-energy in the form of light irradiation above its band gap energy. The holes produced oxidize water directly on the surface of an n-type semiconductor and produce oxygen. The electrons produced move through the external circuit, producing hydrogen at the counter electrode. Therefore, the generated hydrogen and oxygen can easily be separated. In addition, an artificial bias voltage can be applied to the photoelectrode in order to obtain a higher solar-to-hydrogen conversion efficiency [6].

Recently, several groups have focused on the use of TiO_2 nanotubular structures as the water decomposition photoanode. Such a tubular structure increases the light scattering, so that it not only increases the light absorption [7], but also shows a much higher conversion efficiency than TiO_2 nanoparticle-based films, owing to its high electron transporting characteristics. The geometry of TiO_2 nanotube arrays, grown vertically from a substrate, appears to be ideal for water photolysis, allowing for facile electrolyte percolation, due their high surface area, and efficient charge transfer [6].

This study represents the first attempt to make a reactor for hydrogen generation by the photoelectrochemical method using TiO_2 nanotubes as a photoelectrode. The relationship between the amount of hydrogen evolution and three key factors, viz. the tube length, tube structure and crystal structure, was investigated.

2. Experimental

Titanium foils (0.25 mm thick, 99.5% pure) were purchased from Alfa Aesar (Ward Hill, MA). Prior to its anodization, the titanium foil (5.0 cm × 5.0 cm) was ultrasonically cleaned in distilled water and then in acetone for 10 min each. The foil was then dried in an N_2-filled oven. TiO_2 nanotubes were prepared in an aqueous solution made by mixing acetic acid (CH_3COOH (99%, Daejung, Seoul, South Korea)) and 0.5 wt.% hydrofluoric acid (HF (50%, J.T. Baker)) at a concentration ratio of 1:7. The addition of acetic acid results in more mechanically robust nanotubes without changing their shape and size [8,9].

Electrochemical experiments were conducted using a direct current (dc) power supply (VUPOWER AK-6003). A titanium sheet served as the anodic electrode and a platinum electrode as the counter electrode. The samples were anodized at 20 V (15 °C). The

* Corresponding author. Tel.: +82 31 290 7249; fax: +82 31 290 7272.
E-mail address: gyhan@skku.ac.kr (G.Y. Han).

0378-7753/$ – see front matter © 2008 Elsevier B.V. All rights reserved.
doi:10.1016/j.jpowsour.2008.05.059

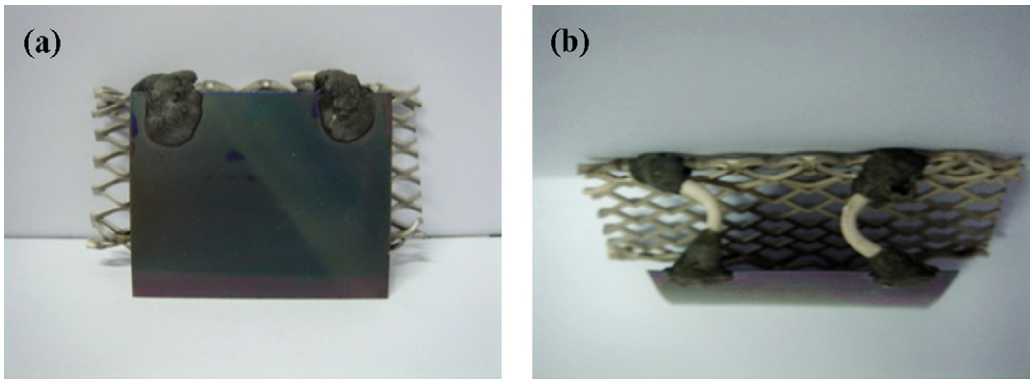

Fig. 1. Images of photoanode connected with counter electrode (a) front side and (b) top side view.

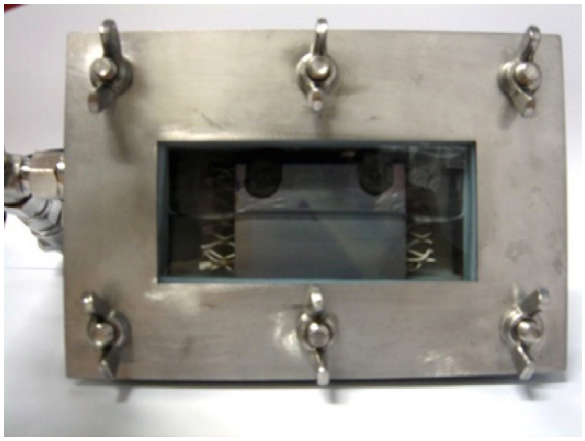

Fig. 2. Image of photocatalytic water-splitting reactor.

nanotubular structure is broken at anodizing voltages greater than 23 V, a sponge-like randomly porous structure being formed [10,11]. The electrolyte temperature has an effect on the wall thickness and tube length: as the temperature increases, a decrease in the wall thickness and tube length was observed [12].

Anodization experiments are commonly conducted with magnetic agitation of the electrolyte, which reduces the thickness of the double layer at the metal/electrolyte interface and ensures a uniform local current density and temperature over the Ti electrode surface [13].

After anodization, they were immediately rinsed with distilled water and then dried in an N_2 stream. They were annealed at 400–600 °C for 6 h with heating and cooling rates of 10 °C min^{-1}. in an O_2 atmosphere to crystallize the tube walls and improve the stoichiometry. Photoelectrochemical cells (PECs) with the TiO_2 photoanode were prepared from the connection between Pt mesh (counter electrode) and Cu wire. Conductive epoxy and nonconductive epoxy cement for metal were used to connect the TiO_2 photocatalyst and Cu wire. The fabricated PEC is shown in Fig. 1.

The reactor made with stainless steel has a volume of 83 mL. The material of the front window of the reactor is quartz glass. The prepared photoelectrode was placed in the reactor and assembled tightly to prevent gas leakage. The electrolyte consisted of 45 mL of 0.01N KOH–1.0 mM KI. Its temperature was about 70 °C. The reactor containing the KOH–KI electrolyte was purged with Ar gas for 30 min and then tightly isolated with a septum. We confirmed that the purge step was fully completed and then started the photoreaction with a 400-W high pressure Hg lamp. The appearance of the device for the experiment is shown in Fig. 2.

3. Results and discussion

Fig. 3(b) and (c) shows the scanning electron microscopy (SEM) images of the surface of the self-organized TiO_2 nanotube arrays and the side view of the TiO_2 nanotube array, respectively. These results show that the TiO_2 nanotubes are well organized vertically and that the tube length is approximately 450 nm after 1 h of anodization. The BET-surface area of the TiO_2 nanotube arrays was determined to be of the order of 11–31 $m^2\,g^{-1}$ by the nitrogen absorption method, which represents the surface of titanium. The TiO_2 nanotube parts were collected from the surface of the as-anodized TiO_2 nanotubes by the stripping method.

The overall mechanism of the anodic formation of straight nanoporous titania can be represented as follows [14,15]:

$$2H_2O \rightarrow O_2 + 4e^- + 4H^+ \quad (1)$$

$$Ti + O_2 \rightarrow TiO_2 \quad (2)$$

$$TiO_2 + 6F^- + 4H^+ \rightarrow TiF_6{}^{2-} + 2H_2O \quad (3)$$

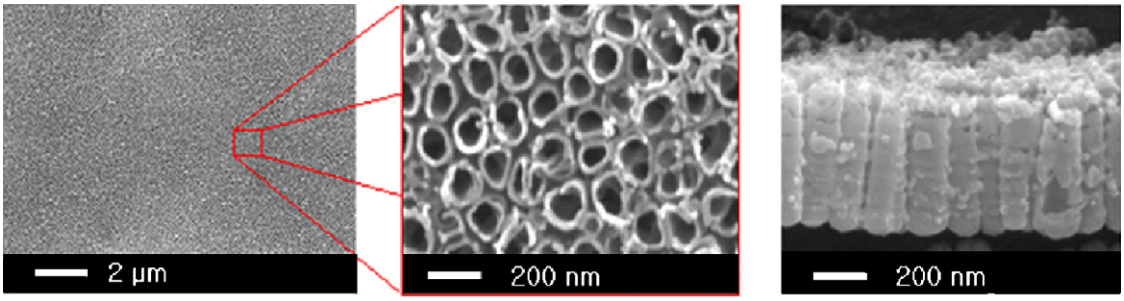

Fig. 3. FE-SEM images of annealed TiO_2 nanotube array: (a) 10,000× top side, (b) 100,000× top side and (c) 100,000× side view of TiO_2 nanotube array.

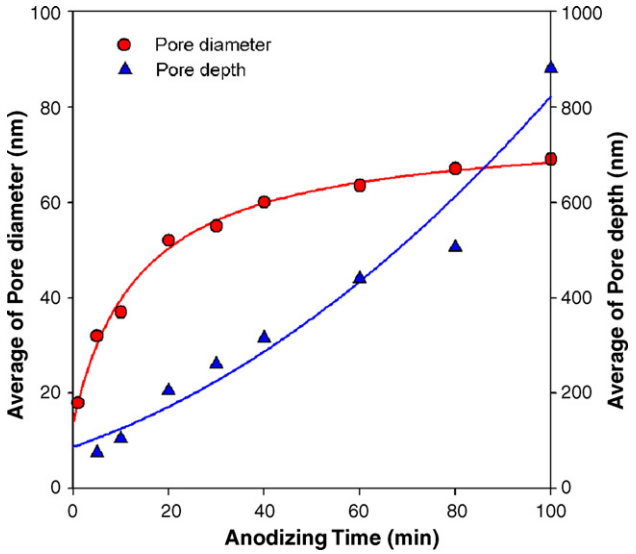

Fig. 4. The average pore diameter and depth as a function of the anodization time.

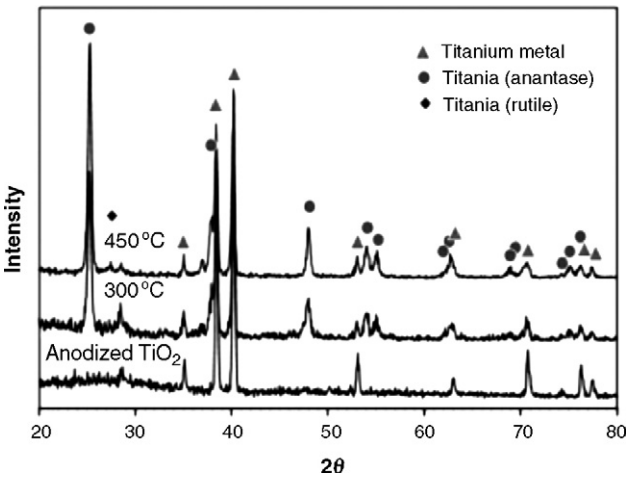

Fig. 6. XRD patterns of the TiO_2 nanotube arrays.

With the onset of anodization, a thin layer of oxide forms on the titanium surface. Small pits originate in this oxide layer, due to the localized dissolution of the oxide, making the barrier layer at the bottom of the pits relatively thin, which, in turn, increases the electric-field intensity across the remaining barrier layer, resulting in further pore growth. The pore entrance is not affected by electric-field-assisted dissolution and hence remains relatively narrow, while the electric-field distribution in the curved bottom surface of the pores causes their widening, as well as their deepening. The result is pores with a scallop shape [14,15]. As the Ti–O bond energy is high (323 kJ mol^{-1}), in the case of titania it is reasonable to assume that only pores having thin walls will be formed, due to the relatively low ion mobility and relatively high chemical solubility of the oxide in the electrolyte, hence unanodized metallic portions can initially exist between the pores. As the pores become deeper, the electric field in these protruded metallic regions increases, enhancing the field-assisted oxide growth and oxide dissolution and, simultaneously, well-defined interpore voids start forming. Thereafter, both voids and tubes grow in equilibrium to yield the final tubular structure [16,17].

An experiment was conducted to determine the average diameter and depth of the nanotube pores as a function of the anodization time. The anodization was applied to the Ti foil for 5–100 min with a voltage of 20 V and, after the anodization, the Ti foil was annealed at a temperature of 400 °C. As the result of the anodization, the conformal formation of nanotubes was identified by SEM (from Fig. 3). The mean pore diameter and depth of the nanotubes obtained from the SEM image is shown in Fig. 4. It was found that the pore diameter of the tubes increased with increasing anodization time up to 40 min., and thereafter remained constant. This means that the anodization time mainly affects the depth of the nanotubes. This is in agreement with the nanotube mechanism mentioned above. First, the pores and voids are formed on the Ti foil surface and after the appropriate settlement of these pores and voids, the development of the tubes proceeds in the longitudinal direction.

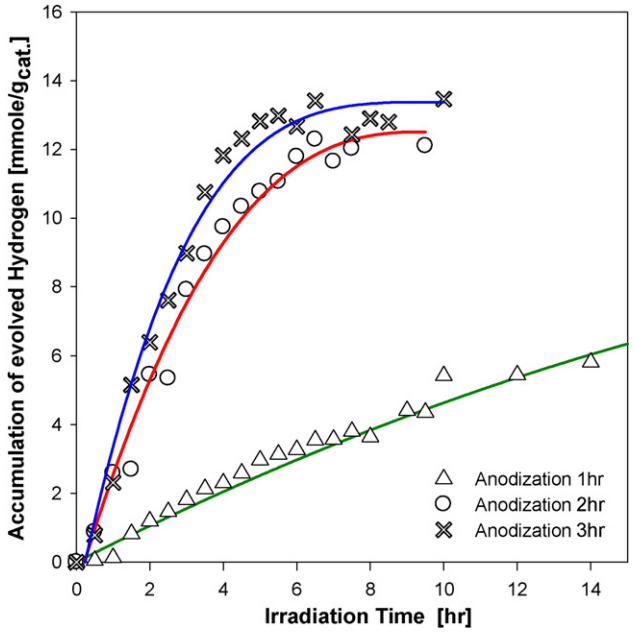

Fig. 5. The amount of hydrogen produced, depending on the anodization time of the photocatalyst.

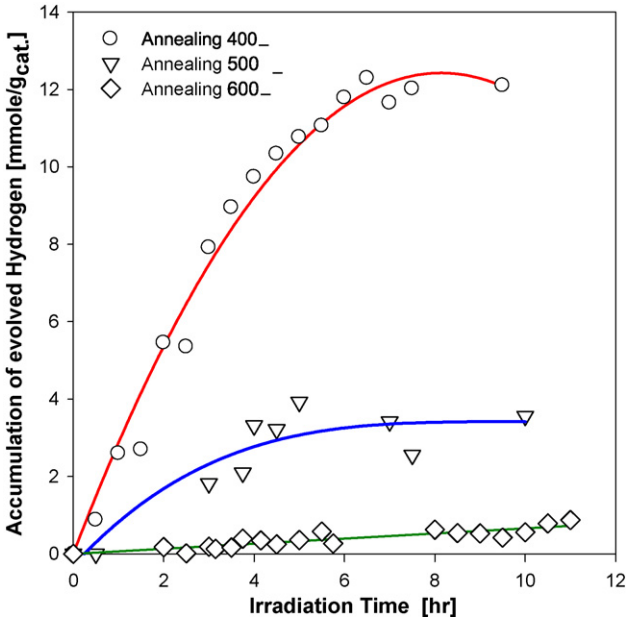

Fig. 7. The amount of hydrogen produced as a function of the annealing temperature.

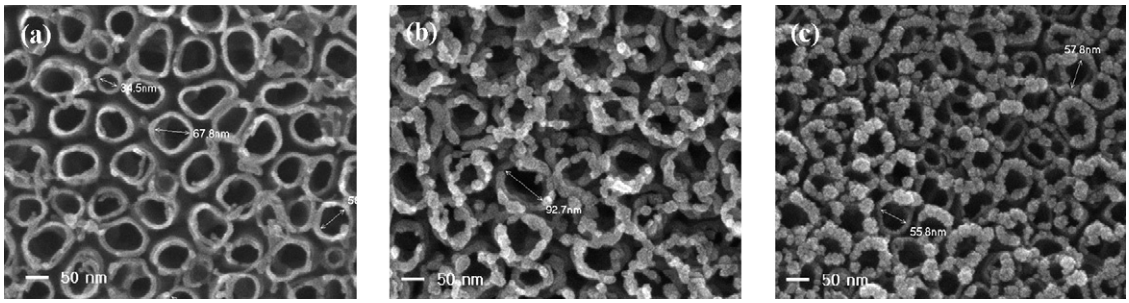

Fig. 8. Top side view (100,000×) FE-SEM images of TiO_2 nanotubes annealed at various temperatures: (a) 400 °C, (b) 500 °C and (c) 600 °C.

It is advantageous to have a larger tube length, because the photocatalyst used for the water-splitting reaction should have a large contact area with the electrolyte. The amount of hydrogen generated increased with increasing anodization time [18], as shown in Fig. 5. If we consider the above relationship between the anodization time and the formation of the TiO_2 nanotubes, we can verify the fact that the amount of generated hydrogen is directly related to the tube length. This means that the contact area between the tubes and electrolyte is an important factor in the evolution of hydrogen. As can be seen in Fig. 5, the effect of the tube length on the hydrogen evolution was diminished at an anodization time of more than 2 h. In addition, the amount of hydrogen evolved became saturated as the irradiation time was increased, especially in the case of the photoanode with a longer tube length. This might be due to the reduction in the iodide concentration with increasing reaction time.

The effects of the annealing temperature on the hydrogen evolution were investigated. The Ti foil was anodized at 15 °C and 20 V for 3 h and then annealed for a further 6 h at a temperature of either 400, 500 or 600 °C. The as-anodized titania nanotubes are amorphous and are subsequently crystallized by the high-temperature annealing. In the present work [19], the anatase phase started to appear at a temperature of 300 °C. A weak rutile phase peak appeared in the X-ray diffraction pattern at a temperature near 450 °C. The XRD patterns of the TiO_2 nanotube arrays annealed at different temperatures in O_2 gas are shown in Fig. 6.

The results of our experiment confirmed the decreasing tendency of the hydrogen generation with increasing annealing temperature (Fig. 7). This was attributed to the fact that as the annealing temperature increases, the disruption of the tubes as well as the breakdown of the inlet of the tubes take place, resulting in particle growth (Fig. 8). This is the main reason for the decrease in the contact area between the tubes and electrolyte during the water-splitting reaction. However, the quality of the crystallized titania will be low if too low an annealing temperature is used [7,20,21]. Therefore, the temperature range of 250 °C (the starting point of anatase formation [7]) to 450 °C (the starting point of tube disruption) is suitable for the manufacture of the photocatalyst.

4. Conclusions

We studied the characteristics of nanotube formation and its relation to hydrogen generation by water splitting as a function of the preparation conditions of the photocatalyst. It was found that the length of the tubes is increased in proportion to the anodization time. However, the pore diameter remained almost constant after an anodization time of 40 min. We also found that the formation of particles on the tube inlet, which is caused by the disruption of the tubes, occurs increasingly often as the annealing temperature increases. We prepared a water-splitting reactor and performed water splitting under these conditions. We verified the effectiveness of the hydrogen generation reaction under the optimized conditions.

Acknowledgments

This research was performed for the Hydrogen Energy R & D Center, one of the 21st Century Frontier R & D program, funded by the Ministry of Education, science and technology of Korea.

References

[1] M. Ashokkumar, Int. J. Hydrogen Energy 23 (1998) 427.
[2] N. Serpone, E. Pelizzetti, Photocatalysis: Fundamentals and Applications, Wiley, New York, 1989.
[3] M. Schiavello, H. Dordrecht, Photoelectrochemistry, Photocatalysis and Photoreactors: Fundamentals and Development, Kluwer Academic Publishers, Boston, 1985.
[4] A.L. Linsebigler, G. Lu, J.T. Yates, Chem. Rev. 95 (1995) 735.
[5] N. Meng, K.H.L. Michael, Y.C.L. Dennis, K. Sumathy, Renew. Sust. Energy Rev. 11 (2007) 401.
[6] F.I. Marin, M.A. Hamstra, D. Vanmaekelbergh, J. Electrochem. Soc. 143 (1996) 1137.
[7] G.K. Mor, O.K. Varghese, M. Paulose, K. Shankar, C.A. Grimes, Solar Energy Mater. Solar Cells 90 (2006) 2011.
[8] G.K. Mor, M.A. Carvalho, O.K. Varghese, M.V. Pishko, C.A. Grimes, J. Mater. Res. 19 (2004) 628.
[9] G.K. Mor, O.K. Varghese, M. Paulose, C.A. Grimes, Sensor Lett. 1 (2003) 42.
[10] D. Gong, C.A. Grimes, O.K. Varghese, W. Hu, R.S. Singh, Z. Chen, E.C. Dickey, J. Mater. Res. 16 (2001) 3331.
[11] G.E. Thompson, R.C. Furneaux, G.C. Wood, J.A. Richardson, J.S. Goode, Nature 272 (1978) 433.
[12] G.K. Mor, K. Shankar, M. Paulose, O.K. Varghese, C.A. Grimes, Nano Lett. 5 (2005) 191.
[13] G. Patermarakis, K. Moussoutzanis, J. Electrochem. Soc. 142 (1995) 737.
[14] V.P. Parkhutik, V.I. Shershulsky, J. Phys. D: Appl. Phys. 25 (1992) 1258.
[15] A. Pakes, G.E. Thompson, P. Skeldon, P.C. Morgan, Corros. Sci. 45 (2003) 1275.
[16] J. Siejka, C. Ortega, J. Electrochem. Soc. 124 (1977) 883.
[17] G.E. Thompson, Thin Solid Films 297 (1997) 192.
[18] M. Paulose, M.G.K. Mor, O.K. Varghese, K. Shankar, C.A. Grimes, J. Photochem. Photobiol. A: Chem. 178 (2006) 8.
[19] W.S. Nam, G.Y. Han, J. Chem. Eng. Jpn. 40 (2007) 266.
[20] O.K. Varghese, D.W. Gong, M. Paulose, C.A. Grimes, E.C. Dickey, J. Mater. Res. 18 (2003) 156.
[21] G.K. Mor, O.K. Varghese, M. Paulose, C.A. Grimes, Adv. Funct. Mater. 15 (2005) 1291.